Science of the Total Environment 784 (2021) 147119

Contents lists available at ScienceDirect

Science of the Total Environment

journal homepage: www.elsevier.com/locate/scitotenv

High-performance low-cost solar collectors for water treatment fabricated with recycled materials, open-source hardware and 3d-printing technologies

Miguel Martín-Sómer, Jose Moreno-SanSegundo, Carmen Álvarez-Fernández, Rafael van Grieken, Javier Marugán *

Department of Chemical and Environmental Technology, ESCET, Universidad Rey Juan Carlos, C/ Tulipán s/n, 28933 Móstoles, Madrid, Spain.

HIGHLIGHTS

- The price of solar collectors can be greatly reduced using 3D printing techniques.
- Cheap 3D printed CPC collector have 80% efficiency compared to a commercial one.
- Open-source hardware is suitable for control strategies in solar collectors.
- UV LED can successfully use to achieve constant reaction rate under solar radiation
- PTC coupled to a solar tracking system improves 280% the efficiency of the CPC.

GRAPHICAL ABSTRACT

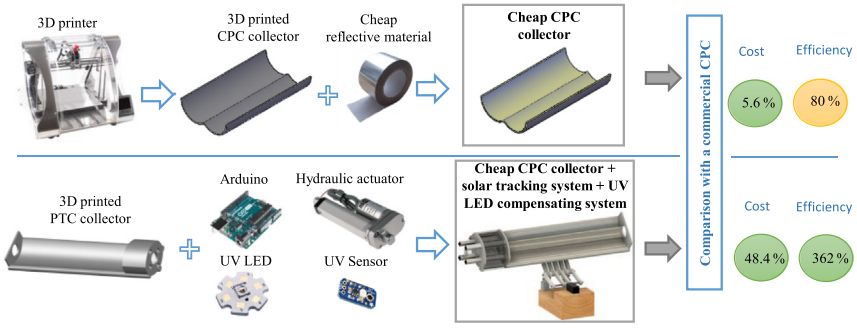

ARTICLE INFO

Article history:
Received 5 February 2021
Received in revised form 7 April 2021
Accepted 9 April 2021
Available online 16 April 2021

Editor: Damia Barcelo

Keywords:
Arduino
Water treatment
Solar reactor
Photo reactor
CPC reactor
PTC reactor

ABSTRACT

Solar technologies constitute an excellent alternative for water treatment in low-income countries where the poverty of a large part of the population hinders their access to safe water. From a technical point of view, the use of compound parabolic collectors (CPC) has been consolidated in the last decades. However, the relatively high cost of tooling conventional manufacturing processes for these collectors makes them difficult to afford in the most impoverished regions. This work presents the development of low-cost CPC and parabolic through solar collectors (PTC) by 3D printing of the structure and the use of recycled reflective materials. Besides, open-source hardware has been used to control system operation, including a supplementary UV LED system to compensate for the operation under low solar irradiance. Regarding the tested reflective materials, an optimum is obtained using an aluminium adhesive sheet that leads to an efficiency of 80% compared to a commercial CPC made of high-quality anodised aluminium, being the cost 20 times lower. On the other hand, incorporating a low-cost solar tracking system in a printed PTC reactor could lead to efficiencies up to 300% compared to the commercial CPC, while the cost was 4.5 times lower. Finally, the LED compensation system was successfully validated, allowing the operation with a constant treatment capacity during operation in cloudy conditions. In conclusion, the developed collectors are high-performance solar water treatment systems with a significantly lower investment cost, making them affordable worldwide.

1. Introduction

Water is a limited resource essential for life and health. In July 2010, the General Assembly of the United Nations recognised through

* Corresponding author.
E-mail address: javier.marugan@urjc.es (J. Marugán).

https://doi.org/10.1016/j.scitotenv.2021.147119

resolution 64/292 the right to drinking water as a fundamental human right (United Nations General Assembly, 2010). However, the availability of water is only legally guaranteed by a few countries. According to a World Health Organization (WHO) report, 29% of the world's population does not have access to drinking water at home (OMS/UNICEF, 2017).

Every year millions of people get diseases such as diarrhoea, cholera, dysentery, typhoid fever and polio because of the intake of water contaminated by pathogens. It is estimated that only diarrheal conditions cause more than 1.8 million deaths per year, of which 526,000 correspond to children under five years (Black et al., 2016). In addition, many water sources are contaminated with heavy metals, chronic organic pollution, and waste materials that have a destructive effect on public health and the environment (Dharwal et al., 2020). The shortage of drinking water is one of the most transcendental problems worldwide, affecting the most disadvantaged population and decreasing their quality of life.

The development of a low-cost water treatment method could contribute to eradicate extreme poverty and alleviate the development of diseases caused by the intake of contaminated water. It is essential to consider that most regions affected by water scarcity, such as sub-Saharan Africa, South Asia, East Asia, or Southeast Asia, usually register high solar irradiance values. Therefore, solar photoactivated processes can be considered a potential cheap solution for water treatment. These processes are based on the use of ultraviolet radiation in sunlight to promote the elimination of pollutants and pathogens. The use of these types of processes, such as the SODIS process, is recommended by the WHO and are used daily by more than 2 million people in 33 countries (Meierhofer and Landolt, 2009).

These processes are economically affordable for most of the world's population due to their low cost (Clasen et al., 2007). They have demonstrated a decrease in the risk of contracting different diseases (McGuigan et al., 2011). However, its use is limited due to the long exposure times required due to limited available UV radiation (Rose et al., 2006). These drawback can be mitigated by increasing the amount of UV radiation delivered to the water. For this purpose, surfaces capable of concentrating solar radiation can be incorporated. Among the most common concentrating systems, the parabolic trough collector (PTC) and the compound parabolic collector (CPC) stand out. The PTC consists of a collector whose reflector follows the shape of a parabola along a cylindrical channel. The radiation is reflected and concentrated towards the receiving tube (through which the water circulates) located in the focal line of the parabola. This type of collector only allows direct solar radiation to be concentrated, so its use is limited to low diffuse radiation conditions. One possibility to maximise concentrated radiation is to attach them to a solar tracking system that maximises the direct solar radiation received (Malato et al., 2009). On the other hand, the CPC is a static collector whose reflective surface is arranged in such a way that the normal at each point of the collector is tangent to the circumference that constitutes the section of the tube. The main characteristic of these collectors is that they can concentrate both direct radiation and diffuse radiation (Malato et al., 2004), so a solar tracking system is not required.

As mentioned above, these collectors increase the incident radiation captured for the process and, therefore, its efficiency. Nevertheless, this improvement also represents a notable increase in the overall cost of the process since the collectors are usually constructed of high-quality aluminium, and the manufacturing to obtain the parabolic shape required to achieve the correct reflection of the Sun's rays is not simple. Consequently, the increase in the cost of water treatment can turn it into an unattainable expense in low-income locations.

The main objective of this work is the development of low-cost parabolic collectors to increase the radiation captured for its use in water treatment processes. The manufacturing of the plastic support for the collectors with the appropriate geometrical shape has been carried out by 3D printing. The reflecting coating has been done using different kind of materials, including recycled ones. The efficiency for radiation collection of the different prototypes has been assessed and compared with a commercial CPC of similar features.

On the other hand, a PTC reactor coupled with a solar tracking system based on open-source hardware was developed and compared with the CPC system, both in terms of performance and cost. Besides, as UV LED have shown great potential for water treatment processes (Martín-Sómer et al., 2018; Martín-Sómer et al., 2019), a UV LED device actuated by the control system were also coupled to study the possibility of carrying out the water treatment in steady-state, regardless of the solar irradiation conditions. This hybrid solar and artificial UV radiation configuration, previously proposed for photobioreactors (Ogbonna et al., 2001, 1999), was applied to photoactivated water treatment processes using solar collectors.

2. Material and methods

2.1. Photoreactors design

For comparison purposes, all photoreactors were based on a borosilicate glass tube of 380 mm in length, 26 mm in inner diameter and 2 mm thickness (0.2 L of irradiated volume). CPC reactors were geometrically designed and sized based on these tube dimensions and a specific concentration factor of 1. The PTC reactor was designed with a radiation collection area equivalent to that of the CPC reactor (358 cm^2). Therefore, an opening width of 81.7 mm and a total length of 380 mm were used. Although the opening width/collector diameter ratio in PTC can reach values up to 82 (Günther et al., 2011), in this case, a much lower value can be used, as water heating is not pursued. Therefore, based on the same tube diameter and radiation collection area, a ratio of 3.1 is obtained. Fig. S1 shows the schematic representation of both the CPC reactor and the PTC reactor.

2.2. Photoreactors manufacturing

Once the design parameters of the photoreactors were established, the reactors were modelled three-dimensionally using CAD software. The software Voxelizer 1.4.13 was used to convert the three-dimensional models to G-code interpretable by the 3D printer (ZMorph VX 3D), and the printing parameters were established. Polylactic acid (PLA) was chosen as printing material, using a melting temperature of 220 °C, a layer thickness of 0.2 mm and a temperature for the printer's base of 60 °C. To balance the consumption of PLA and the collectors' resistance, the interior of the collectors' structure was 10% filled with a rectangular mesh (Fig. 1). The printing time required to manufacture the CPC reactor was 33.25 h, while the time needed to print the PTC was 22.48 h. These time values could be indeed reduced through the optimisation of the printing parameters, but this was out of the scope of this work.

Once the plastic supports for the collectors were fabricated, they were coated with different reflective materials to concentrate the solar radiation on the reactor tube (Fig. S2). Since the main objective of the work is to design low-cost solar reactors, cheap and even recycled materials were chosen. The materials selected for the study were: steel soda can, aluminium soda can, aluminium foil adhesive tape and adhesive acrylic mirror sheet. The reflectivity of these materials was measured using a Varian Cary 500 model UV–Vis-NIR spectrophotometer coupled to an integrating sphere. In the case of the commercial CPC, the surface of the reflector is made of high quality anodised aluminium that guarantees an 85% direct light reflection.

2.3. Solar tracking system

Two light-dependent resistors (LDR, DealMux GL5539 30 K-90 KOhm 150 V LDR) were attached to the PTC collector, as shown in Fig. 2. These sensors are tilted 45° respect the opening area and record the radiation reaching each side of the reactor. An open-source control board (Arduino UNO) was used to compared both results (using **code S1** in the supplementary information). If the registered data does

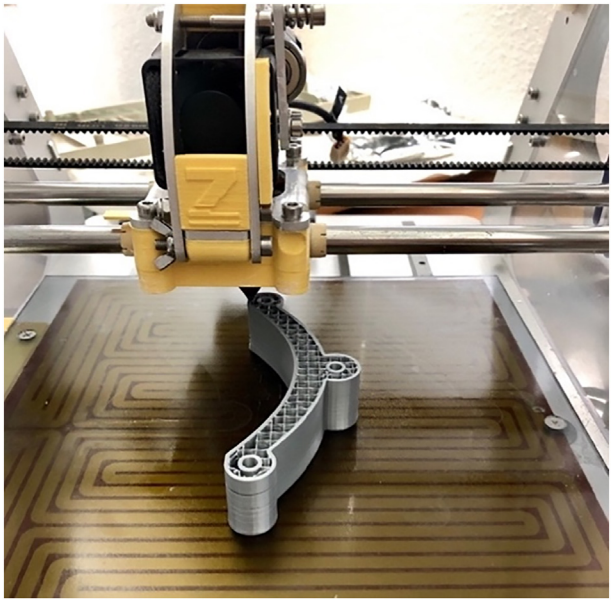

Fig. 1. 3D printing of the support of the PTC reactor.

not have a similar value, it means that the solar rays are not reaching perpendicular to the collector's surface. In this case, using a hydraulic linear actuator, the collector was rotated towards the sensor with the highest irradiance value until the signals recorded in both sensors equals. A Neuftech L298N motor controller module was used to modify the position of the linear actuator from the control board.

2.4. Supplementary UV LED system

An artificial UV illumination system was coupled to the PTC to ensure that the UV radiation reaching the reactor tube was controlled regardless of the solar radiation conditions. This system consists of four squared aluminium bars with two UV 365 nm LEDs (LedEngin Model LZ1- 00UV00), each one placed symmetrically to the centre of the receiver tube. This ensures a relatively homogeneous distribution of the emitted radiation, which is a critical factor in maximising efficiency (Martín-Sómer et al., 2017). The UV radiation reaching the reactor was measured using an Adafruit GUVA-S12SD UV sensor. **Code 2** in the supplementary information details the control strategy, based on establishing the threshold incident radiation value to carry out the water treatment effectively. The UV sensor collects the solar radiation that reaches the reactor. Based on this measurement, the electrical intensity fed to the LED is controlled to get the required emission to reach the threshold incident radiation value.

2.5. Experimental methods

All the photoreactors have been operated in recirculation mode with a reservoir tank, using a total volume of 2 L of water. The flow rate was 12.3 L/min, driven by a centrifugal pump. For experiments with artificial light, a large scale solar simulator with a 6000 K xenon lamp (Osram XBO 5000 W / H XL OFR) was used, being the collectors surface perpendicular to the direction of the light. A schematic representation of the experimental set-up and the spectral distribution of the solar simulator can be found elsewhere (Philippe et al., 2016). On the other hand, the experiments under natural sunlight were carried out with the fixed collectors tilted 40° to the South, corresponding to the local latitude of Universidad Rey Juan Carlos facilities in Móstoles, Spain (40.33°N, 3.86°W) (Fig. 3). To compare the performance of the different reactors and reflective materials, potassium ferrioxalate actinometry experiments were carried out following the procedure described elsewhere (C G Hatchard and Parker, 1956). These experiments allowed the calculation of the amount of radiation reaching the borosilicate tube in each studied case. Long-term photocatalytic experiments of methanol oxidation (Sigma-Aldrich) were carried out to study the solar tracking system and the artificial UV lighting systems coupled to the PTC. The photocatalytic experiments were carried out using commercial Evonik P25 titanium dioxide as photocatalyst at a concentration of 0.1 g/L, previously optimised (van Grieken et al., 2009). An initial methanol concentration of 100 mM was fixed according to previous studies [16,17]. Methanol oxidation was followed through the colourimetric determination of the formaldehyde produced throughout the reaction, quantitative oxidation product with methanol in excess (Pablos et al., 2014).

Although the intrinsic kinetics of the photocatalytic process does not depend on the reactor and collector system, the experimental formation of formaldehyde is directly conditioned by the efficiency in the collection of UV photons. Therefore, the comparison of the efficiency of the different solar collectors was carried out in terms of the apparent formaldehyde production rate as a function of the solar irradiance received at

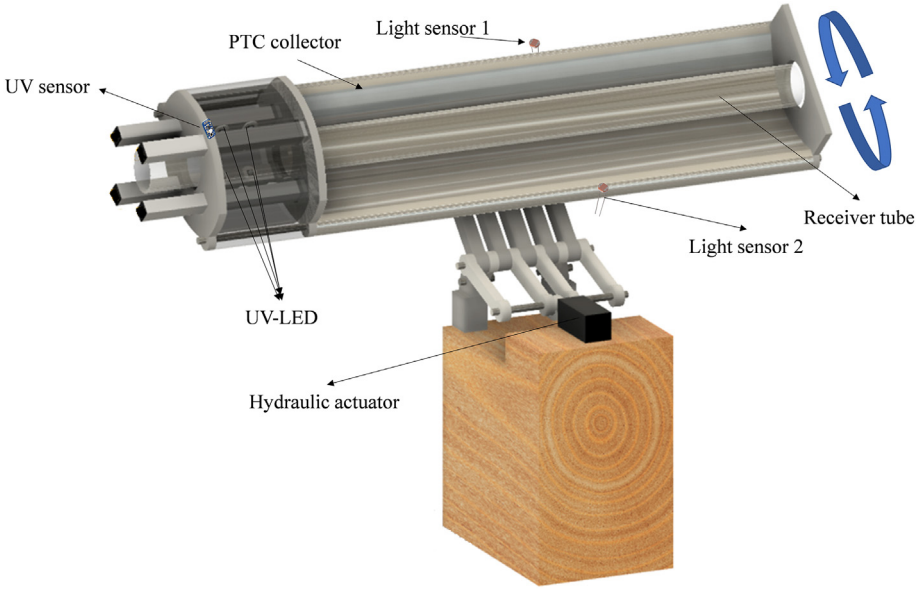

Fig. 2. Schematic representation of the PTC reactor coupled to a solar tracking system and UV artificial lighting system.

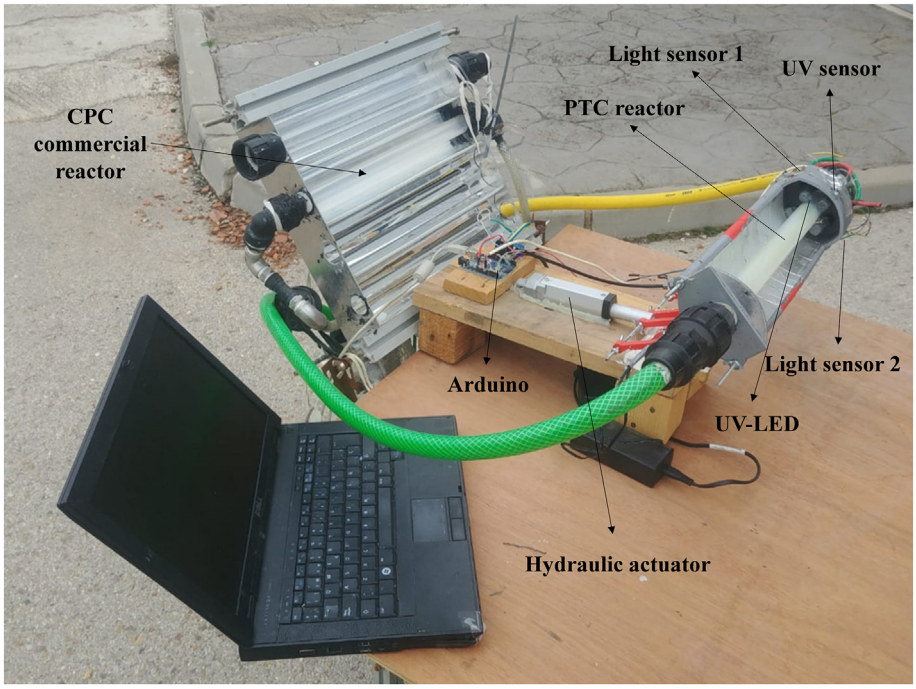

Fig. 3. Image of the photocatalytic experiments carried out simultaneously under solar irradiation with both a commercial CPC reactor and a 3D printed CPC reactor.

the Earth surface. The solar UV dose was calculated from solar radiation flux measurements using a PCE-UV34 radiometer. Quantitative formaldehyde production rate values in mmol/kJ were calculated considering the collector surface area (0.049 m^2) and the total water reaction volume (2 L).

3. Results

3.1. Reflectivity of the materials

The optical properties of the reflective materials play an essential role in the efficiency of solar light use. It is especially important to analyse their reflectivity in the ultraviolet range of the solar spectrum (300–400 nm), as it determines the incident radiation available for the activation of the photochemical processes in the reactor tube. The spectral reflectance (ratio of reflected radiation to incident radiation) of the studied materials (Fig. 4) was measured using a spectrophotometer coupled to an integrating sphere. In all cases, the reflectance values are lower than the theoretical value corresponding to high-quality anodised aluminium (approx. 85%) (Fend et al., 2000). The aluminium foil adhesive tape presents a remarkable reflectance of near 70% in the whole studied range from 250 to 800 nm. The adhesive acrylic mirror sheet also shows a reflectance near 70% in the visible and UV-A range but shows a significant decrease in reflectance in the UV-B range. For aluminium soda cans, although it shows a lower reflectance, it keeps a reflectance close to 50% in the UV region and the non-reflective threshold is observed at a lower wavelength, showing a better performance than the mirror sheet in the UV-B region. Therefore, it can be considered an interesting alternative, especially considered as a cheap reused waste. The steel soda can shows the lowest reflectance values, below 40% in the whole studied range and with an average value in the UV region of around 20%.

3.2. Optical performance of the developed CPC reactors

The efficiency of any photochemical process in the reactor depends on the incident radiation inside the tube. Therefore, the optical performance of the 3D printed CPC covered with the different reflective materials was evaluated by actinometry. The same experiment was also carried out with the commercial CPC of high-quality anodised aluminium for comparative purposes. Fig. 5 shows the formation of Fe^{2+} versus time throughout the actinometric reactions. The results obtained were adjusted linearly, and the slope was obtained. Since the quantum yield of the potassium ferrioxalate actinometry is known, it is possible to get the total incident radiation reaching the reactor tube from the slope. As the quantum yield depends on the wavelength (Goldstein and Rabani, 2008), the total incident radiation was estimated considering a quantum yield of 1.273 mol/Einstein, the weighted averaged value for the solar simulator's emission spectrum. The photon flow calculated for the commercial CPC reactor was 1.56×10^{-5} Einstein/s, whereas, for the 3D printed reactor, the results were 0.60×10^{-5}, 1.0×10^{-5}, 1.26×10^{-5} and 1.10×10^{-5} Einstein/s for the steel soda can, aluminium soda can, aluminium foil adhesive tape and adhesive acrylic mirror sheet reflective materials, respectively.

The aluminium foil adhesive tape showed the highest efficiency in light concentration from the studied materials, reaching 80% of the

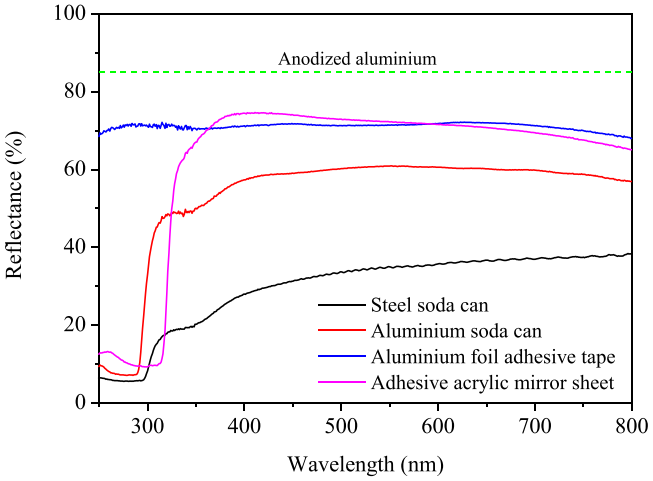

Fig. 4. Spectral reflectance of the studied materials.

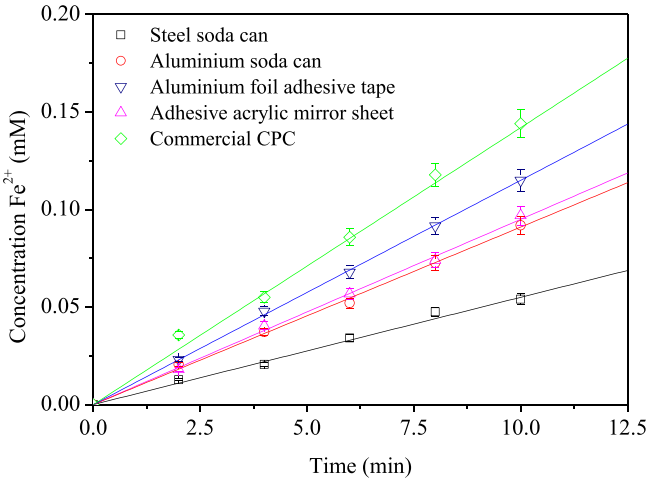

Fig. 5. Results of the potassium ferrioxalate actinometry experiments for a commercial CPC reactor and the 3D printed CPC reactors coated with different reflective materials.

efficiency of the high-quality anodised aluminium. This is a very promising result, as this moderated decrease in light concentration efficiency can be counteracted by a significant drop-off in the reactor's cost, as analysed in Section 3.4. In terms of global optical efficiency, the following material was the adhesive acrylic mirror sheet, showing 68% of the high-quality anodised aluminium's efficiency. However, as previously shown, the reflectance of this material in the UV-B region is limited, and therefore also its application for some photochemical and photocatalytic processes such as solar water disinfection, where direct UV-B radiation absorption is the main mechanism responsible for the bacterial damage. This high value for the global reflectivity is due to the high spectral reflectance in the UV-A and near UV visible range, as potassium ferrioxalate actinometer absorbs wavelengths up to 510 nm (C. G. Hatchard and Parker, 1956).

On the other hand, it is important to note that the aluminium soda can achieve 63% of anodised aluminium's efficiency. Although, in this case, its reflectivity was less than that of the aluminium foil adhesive tape, the use of this recycled material could still be considered as a coating material for low-cost CPC reactors for applications not exclusively based on UV-B light, similarly to the adhesive acrylic mirror sheet. Finally, as expected from the reflectance spectra shown in Fig. 4, the efficiency of the steel soda can is much lower (38% with respect to the anodised aluminium), and it is also not able to reflect UV-B radiation. Considering these results, the aluminium foil adhesive tape was chosen as coating material for the 3D printed plastic structures. This type of material has also been suggested by other authors (Zheng et al., 2020).

Finally, it is worth mentioning that, although the long-term durability of the materials has not been evaluated, all of them were originally designed for durable applications, and therefore, a sufficiently high lifespan is expected. In any case, its replacement would be easy and cheap.

3.3. Evaluation of low-cost 3D printed PTC

The previous section showed how a 3D printed reactor coated with a cheap reflective material could obtain optical efficiencies of up to 80% compared to a commercial reactor with high-quality anodised aluminium. This section analyses in comparative terms the efficiency of a 3D printed PTC reactor coated with the same reflective layer under sunlight. Additionally, the coupling to the PTC of an open-source hardware based solar tracking system and a UV radiation compensation system is analysed.

In this case, the fast actinometry measurement is not suitable for quantifying the effect of solar tracking and UV compensation systems, as their potential advantages can only be captured in longer photochemical experiments. The efficiency of the developed systems was evaluated using the photocatalytic oxidation of methanol as UV-A activated test reaction.

First, both reactors' performance was compared in a fixed position tilted 40° (local latitude) to the South, as shown in Fig. S3.

Fig. 6 shows a higher formaldehyde production rate when using the fixed PTC reactor than the fixed CPC reactor for equivalent collection area and tube diameter. In theory, the opposite behaviour would be expected, as the CPC can concentrate sunlight of any beam angle. In contrast, the PTC only capture beam angles close to the direction perpendicular to the collection surface. However, it has to be noted that the

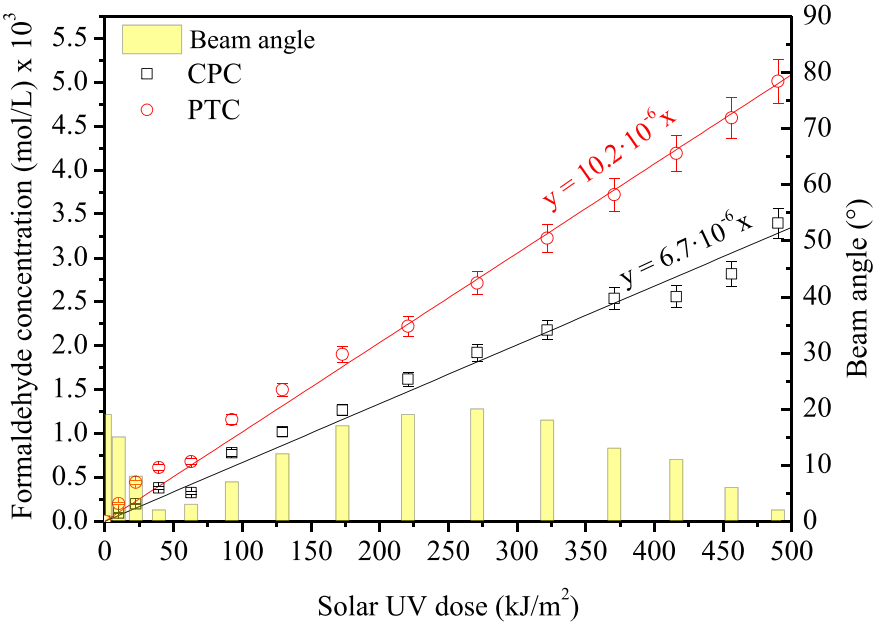

Fig. 6. Formaldehyde formation during the photocatalytic oxidation of methanol in a commercial CPC reactor and a 3D printed PTC reactor, both tilted 40° to the South. Beam angles calculated from the solar vector along the experiment, carried out at 40.33°N, 3.88°W in July 2020 between 10:00 am and 5:00 pm Solar UV dose calculated from the solar radiation flux at the horizontal plane.

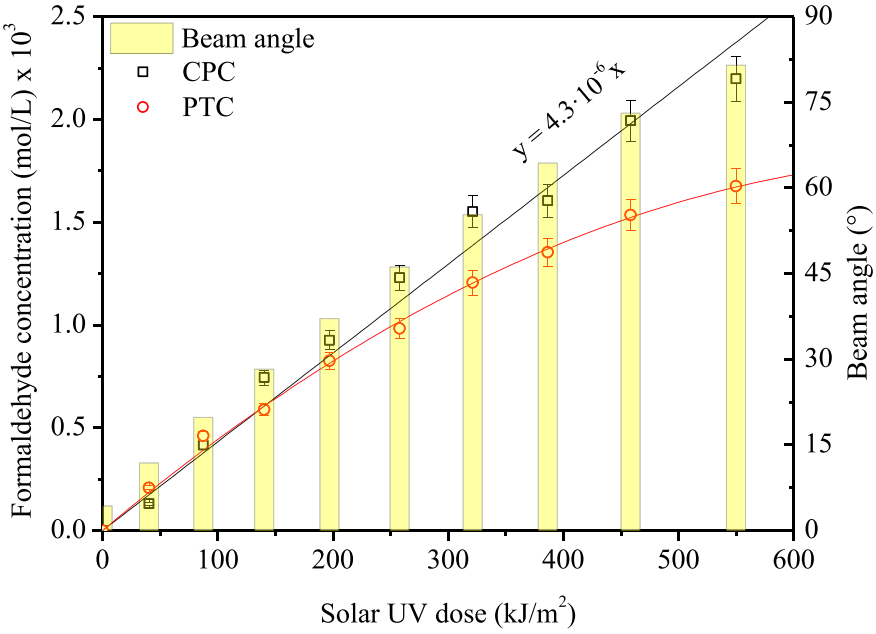

Fig. 7. Formaldehyde formation during the photocatalytic oxidation of methanol in a commercial CPC reactor and a 3D printed PTC reactor, both tilted 90° to the East. Beam angles calculated from the solar vector along the experiment, carried out at 40.33°N, 3.88°W in July 2020 between 10:30 am and 3:30 pm. Solar UV dose calculated from the solar radiation flux at the horizontal plane.

designed PTC reactor has an opening area/tube diameter ratio that allows the concentration of solar rays of up to 30%. Consequently, as both collectors are reflecting all the incident radiation to the reactor, and they have identical collection area and tube diameter, similar results are expected. However, due to the collectors' geometry, at low beam angles, the radiation bounces more times in the CPC than in the PTC, losing energy due to the non-ideal reflection. Moreover, the average radiation pathway across the reactor is longer in the PTC, as all rays are crossing the tube centre with a diameter chord, while rays in the CPC cross the tube following shorter chords (Fig. S4). In processes with low or medium optical density, the path length strongly affects the absorbed energy, and thus, the reaction kinetic. Therefore, for experiments conducted in the summer season where the beam angle takes values below 20° during the whole reaction (Fig. 6), the PTC reactor is even more efficient than the CPC reactor, with formaldehyde production rates of 0.42 and 0.27 mmol/kJ, respectively.

To be able to study the efficiency of both reactors when solar rays reach them with higher beam angles (as would happen in other seasons of the year), the reactors were set with an unusual orientation tilted 90° to the East. In this way, since the Sun's path follows an East-West

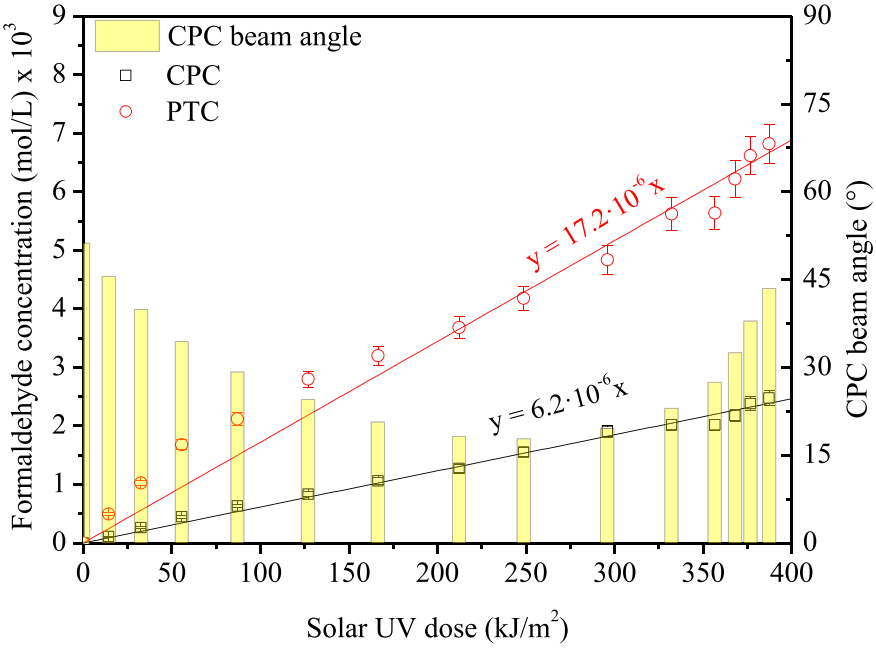

Fig. 8. Formaldehyde formation during the photocatalytic oxidation of methanol in a commercial CPC reactor (tilted 40° to the South) and a 3D printed PTC reactor coupled with a solar tracking system. CPC beam angles calculated from the solar vector along the experiment, carried out at 40.33°N, 3.88°W in September 2020 between 10:30 am and 5:30 pm. Solar UV dose calculated from the solar radiation flux at the horizontal plane.

trajectory, it was possible to get data with beam angles ranging between 0 and 80° along the experiment. Fig. 7 shows the results of formaldehyde formation as a function of the UV solar dose and the corresponding variation of the beam angle. It can be observed that despite the change in the direction of the incident light, the CPC reactor shows a constant formaldehyde production rate of 0.18 mmol/kJ throughout the experiment. In contrast, the PTC reactor presents a slightly higher formaldehyde production rate than the CPC reactor in the first part of the experiment (low beam angles). The production rate decreases as the beam angle increases, becoming a much less efficient reactor.

In summary, it is demonstrated that the 3D printed PTC reactor could reach higher efficiencies than the commercial CPC reactor, but only when it is directly oriented to the Sun. Therefore, the potential incorporation of a low-cost solar tracking system coupled to the PTC is especially interesting.

3.3.1. Evaluation of low-cost 3D printed PTC coupled to a solar tracking system

The coupling of a solar tracking system based on a low-cost open-source control board allows the PTC operation with a constant beam angle perpendicular to the collection area regardless of the inclination of the Sun's rays depending on the location and season of the year. Comparative evaluation of the prototype was carried out with respect to the commercial CPC reactor in the standard inclination of the local latitude (40° N) facing South. The PTC reactor was placed with its axis in the north-south plane to operate following the solar east-west trajectory. As shown in Fig. 8, thanks to the solar tracking system, the formaldehyde production rate of the PTC reactor remained constant throughout the experiment with a value of 0.7 mmol/kJ, improving the efficiency significantly in comparison with the fixed PTC. Additionally, it is verified how the incorporation of the solar tracking system leads to a significant

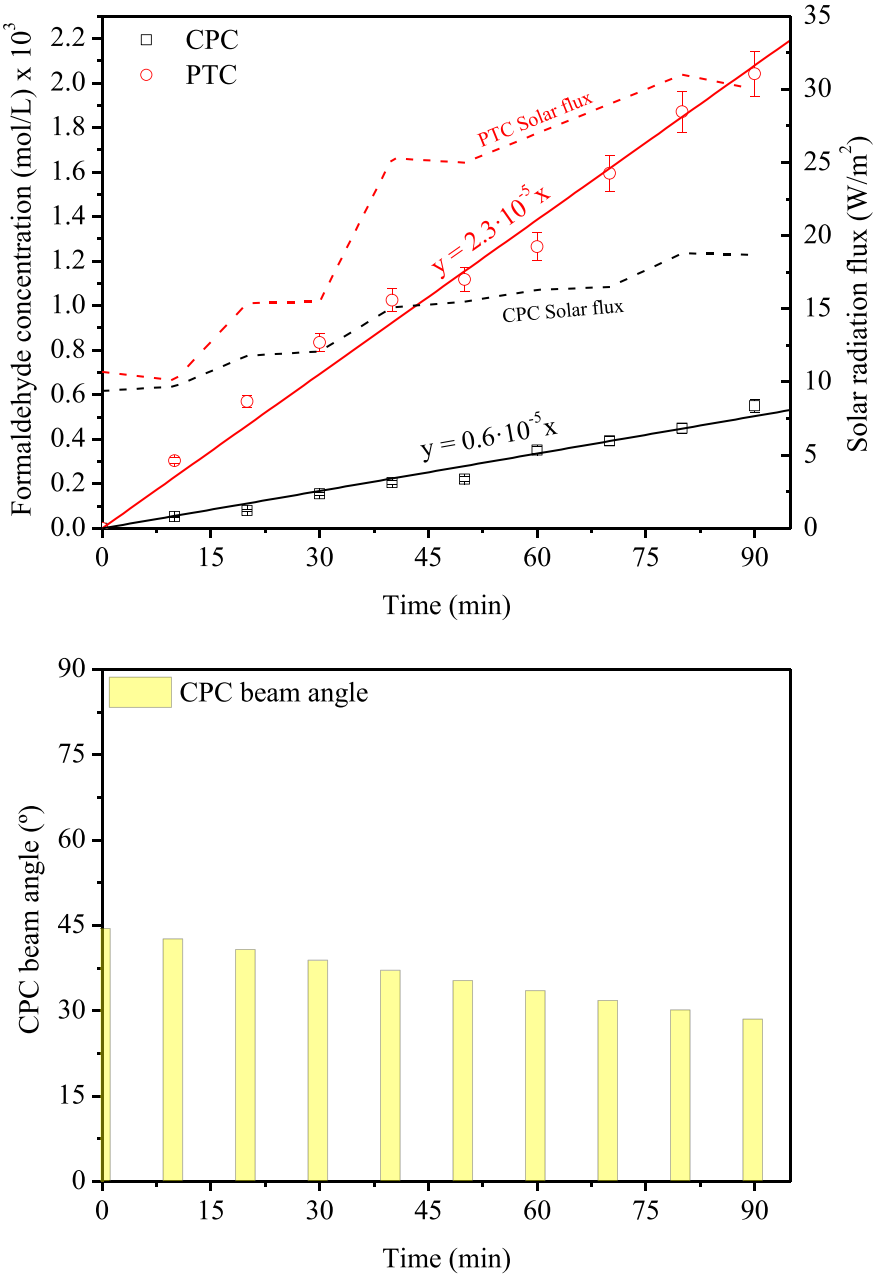

Fig. 9. Formation of formaldehyde vs time during methanol oxidation in a commercial CPC reactor (tilted 40° to the South) and a 3D printed PTC reactor coupled to a solar tracking system and a supplementary UV LED compensation system (top). CPC beam angles calculated from the solar vector along the experiment, carried out at 40.33°N, 3.88°W in July 2020 between 11:10 am and 12:40 pm Solar radiation flux measured at the collector surface plane (bottom).

improvement in the performance of the PTC reactor, showing an efficiency 2.8 times higher than the CPC reactor, with a formaldehyde production rate of 0.25 mmol/kJ similar to the value of 0.27 shown in the experiment in Fig. 6. Similar results when comparing the efficiency of CPC and PTC collectors for a given collector area were reported in the work from Bandala and Estrada (Bandala and Estrada, 2007).

3.3.2. Evaluation of low-cost 3D printed PTC coupled to a supplementary UV LED system

Finally, the possibility of coupling the PTC reactor with a supplementary UV LED system was studied. This system aims to provide additional energy when the available solar UV radiation is not enough to carry out the process. It allows keeping a constant reaction rate regardless of the weather conditions. The emission of the 8 UV LEDs was calibrated by actinometry measurements under increasing input electrical power. The UV sensor was also calibrated with controlled incident UV light intensities using a solar simulator. The system's operation is based on the controlled emission of UV light by the LED system until reaching the incident radiation setpoint set for the reactor if the available sunlight measured by the UV sensor is not enough.

Validation of the supplementary LED lighting system's correct operation was carried out on a partially cloudy day, also comparing its performance with the commercial CPC. Fig. 9 shows a linear production of formaldehyde with time in the PTC system as a result of the solar tracking system (which makes that solar radiation reaches the collector surface always perpendicular, independently of the beam angle) and to the supplementary UV lighting system (which compensates the lower radiation initially received due to the presence of clouds). In the case of the CPC reactor, since the solar radiation was not constant throughout the experiment, a change in the formaldehyde production rate should be observed. However, since the change was not significant, and the CPC is also able to concentrate diffuse radiation, a linear trend is also observed. For this same experiment, Fig. 10 shows the formaldehyde formation versus the solar UV dose. The distribution of solar UV and LED UV reaching the PTC reactor along the reaction is also included. It can be seen how, initially, the supplementary LED lighting system provides a large part of the radiation received. In contrast, in the second part of the reaction, the LED system works at very low power, as the available solar UV radiation was enough to get the value of 30 W/m^2 of UV fixed as a setpoint to carry out the reaction. As a result, two different slopes are clearly observed. In the first part of the reaction, when the LED system operates at high intensity, the formaldehyde production rate is significantly higher than expected (2.18 mmol/kJ) due to the contribution to the total radiation of the UV LED, not taken into account in the solar dose (x-axis). In the second part of the reaction, this slope is not so high because the LED system contribution is negligible, and the solar UV light drives the reaction. In this second section, the PTC's formaldehyde production rate is 0.90 mmol/kJ, 2.91 times higher than with the commercial CPC. This value is in the range of that observed in Fig. 8 when only the solar tracking system was used. In contrast, if both reactors are compared considering the whole reaction (Fig. 9), it can be observed that the overall efficiency of the PTC with the solar tracking system and the supplementary UV LED system improves 3.62 times the efficiency of the commercial CPC reactor.

It is worth noting that the coupling of the UV LED system to the CPC would lead to similar conclusions regarding the adaptation of the process to variable solar irradiance conditions. The main reason to choose the PTC for the proof of this concept is that it already incorporated the control board and automation system for solar tracking.

3.4. Cost analysis

This section analyses the different costs associated with the studied reactors, as the main goal of this work is to develop low-cost solar collectors. To simplify the analysis, only the direct costs of the reactors' components and their manufacturing process have been considered, neglecting staff costs. For the commercial CPC reactor, the costs have been obtained from the work of Miralles-Cuevas et al. (Miralles-Cuevas et al., 2016), using the rule of six tenths (Seider et al., 2004) according to Sánchez Pérez et al. (Sánchez Pérez et al., 2013). The final cost of the commercial CPC reactor used in this work was estimated at 417.4 €. On the other hand, for the economic evaluation of the 3D printed reactors, the total costs were divided into three categories: PLA cost, energy costs and other costs that included screws, nuts, joints, the reflector material and the borosilicate tube (Table S1). In PTC reactors with solar tracking and artificial UV lighting, the additional costs were included in separate categories. Table 1 summarises the costs of each reactor annualised in 10 years, also considering the operating costs associated with the energy

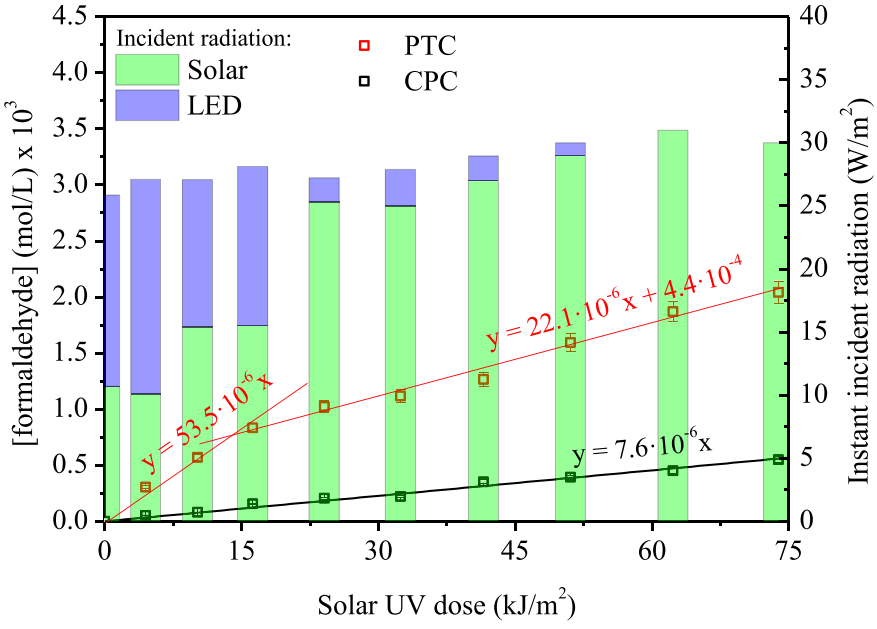

Fig. 10. Formation of formaldehyde vs solar dose during methanol oxidation in a commercial CPC reactor and a 3D printed PTC reactor coupled to a solar tracking system and a supplementary UV LED compensation system. Experiment carried out at 40.33°N, 3.88°W in July 2020 between 11:10 am and 12:40 pm Solar UV dose calculated from the solar radiation flux at the horizontal plane. Instant incident radiation calculated from actinometry experiments.

Table 1
10 years annualised cost of the studied reactors.

	Commercial CPC	CPC	PTC	PTC + Solar tracking	PTC + Solar tracking + UV LED (8 h)	PTC + Solar tracking + UV LED (12 h)	PTC + Solar tracking+ UV LED (16 h)
Investment cost (€)	417.4	23.2	17.5	96.8	185.2	185.2	185.2
Investment cost per year (€)	41.74	2.32	1.75	9.68	18.52	18.52	18.52
Energy consumption per year (kWh)	0.00	0.00	0.00	0.15	7.48	14.95	22.43
Energy cost per year (€)	0.00	0.00	0.00	0.02	1.67	2.50	3.33
10 years annualised cost (€)	41.74	2.32	1.75	9.70	20.19	21.02	21.85
Efficiency ratio vs commercial CPC (%)	100	80	–	280	362	362	362
Cost ratio vs commercial CPC (%)	100	5.6	4.2	23.2	48.4	50.4	52.3

consumption of the solar tracking system and the supplementary UV LED system. The energy consumption of the solar tracking system was estimated considering that the linear actuator performs its full movement twice a day. For the energy consumption of the artificial lighting system, three different scenarios were considered for different solar irradiation conditions in which the artificial UV system operate with an average power of 0.64 W (corresponding to the set point of 30 W/m^2 UV in the receiver tube) for 8, 12 and 16 h per day.

It can be observed how the total cost of the 3D printed CPC reactor was 23.2 €, which represents only 5.6% of the commercial CPC reactor. Therefore, whereas the reduction in efficiency is only 20% (Section 3.2), the cost reduction is almost 95%. Consequently, despite requiring some extra surface for solar collection, the economic efficiency is considerably higher, and the photochemical efficiency significantly higher for the same investment cost.

Regarding the PTC reactor, as shown in Table 1, the annualised cost obtained is only 4.2% compared to the commercial CPC. However, this type of reactor is only suitable if fitted to a solar tracking system, as previously discussed. In such a case, the annualised cost increases to 23.2% with respect to the commercial CPC. Therefore, although the cost reduction is 4–5 times, the increase in efficiency is almost 300%, making the economic efficiency of this system extremely interesting. On the other hand, when the supplementary UV LED system is coupled, the reaction efficiency could be further improved over the commercial CPC by 362% (in the solar irradiation conditions in which the experiment was carried out), whereas the cost remained at 48.4, 50.4 and 52.3% for the 8, 12 and 16 h/day scenarios respectively. These results are very encouraging since, in addition to producing significant efficiency improvements, this system allows for continuous processes using sunlight when available and the LED system when required.

As a summary of this basic economic evaluation, it can be concluded that the aim of developing low-cost solar collectors has been successfully achieved. This is especially relevant considering that the estimated cost for the 3D printed reactors are conservative, and they can be significantly reduced by massive production technologies and the purchase of large quantities of system components.

4. Conclusions

The main conclusion of the present work is that it is possible to manufacture low-cost solar collectors through 3D printing techniques and cheap and even reused reflective materials. The results showed optical efficiencies of up to 80% compared to high-quality anodised aluminium CPC reactors, while the cost was only 5%. These results suggest that this manufacturing technique has great potential to achieve a broader implementation of solar water treatment systems in low-income environments worldwide.

On the other hand, it was possible to verify how open-source control boards allow creating a reliable and low-cost solar tracking system for a PTC reactor that increased the efficiency almost 300%, keeping the cost at 23%. Additionally, an automatically controlled supplementary UV LED radiation compensation system can be successfully applied in an economically profitable way representing an interesting alternative when keeping a constant operation capacity is required, regardless of weather conditions.

CRediT authorship contribution statement

Miguel Martín-Sómer: Investigation, Formal analysis, Writing – original draft. **Jose Moreno-SanSegundo:** Investigation, Data curation, Methodology, Writing – review & editing. **Carmen Álvarez-Fernández:** Investigation, Methodology, Writing – review & editing. **Rafael van Grieken:** Conceptualization, Supervision, Validation, Writing – review & editing. **Javier Marugán:** Conceptualization, Supervision, Funding acquisition, Validation, Writing – review & editing.

Declaration of competing interest

The authors declare that they have no known competing financial interests or personal relationships that could have appeared to influence the work reported in this paper.

Acknowledgements

The authors gratefully acknowledge the financial support of Comunidad de Madrid and European Structural Funds [FOTOCAOS project, Y2018/EMT-5062] and the European Union's Horizon 2020 research and innovation programme in the frame of the PANIWATER project (GA 820718), funded under the Indo-EU International Water cooperation sponsored jointly by European Commission and Department of Science and Technology, India.

Appendix A. Supplementary data

Supplementary data to this article can be found online at https://doi.org/10.1016/j.scitotenv.2021.147119.

References

Bandala, E.R., Estrada, C., 2007. Comparison of solar collection geometries for application to photocatalytic degradation of organic contaminants. J. Sol. Energy Eng. Trans. ASME 129, 22–26. https://doi.org/10.1115/1.2390986.

Black, R., Laxminarayan, R., Temmerman, M., Walker, N., 2016. Disease Control Priorities: Reproductive, Maternal, Newborn and Child Health (Washington DC).

Clasen, T., Haller, L., Walker, D., Bartram, J., Cairncross, S., 2007. Cost-effectiveness of water quality interventions for preventing diarrhoeal disease in developing countries. J. Water Health, 599–608 https://doi.org/10.2166/wh.2007.010.

Dharwal, M., Parashar, D., Shehu Shuaibu, M., Garba Abdullahi, S., Abubakar, S., Baba Bala, B., 2020. Water pollution: effects on health and environment of Dala LGA, Nigeria. Mater. Today Proc. https://doi.org/10.1016/j.matpr.2020.10.496.

Fend, T., Jorgensen, G., Küster, H., 2000. Applicability of highly reflective aluminium coil for solar concentrators. Sol. Energy 68, 361–370. https://doi.org/10.1016/S0038-092X(00)00027-X.

Goldstein, S., Rabani, J., 2008. The ferrioxalate and iodide – iodate actinometers in the UV region. J. Photochem. Photobiol. A Chem. 193, 50–55. https://doi.org/10.1016/j.jphotochem.2007.06.006.

Günther, M., Joemann, M., Csambor, S., 2011. Parabolic Trough Technology, Advanced CSP Teaching Materials, German Aerospace Center (DLR) – Solar Research (Cologne, Germany).

Hatchard, C G, Parker, C.A., 1956. A new sensitive chemical actinometer. II. Potassium ferrioxalate as a standard chemical actinometer. Proc. R. Soc. London. Ser. A. Math. Phys. Sci. 235, 518 LP – 536. doi:https://doi.org/10.1098/rspa.1956.0102.

Malato, S., Blanco, J., Maldonado, M.I., Fernández, P., Alarcón, D., Collares, M., Farinha, J., Correia de Oliveira, J., 2004. Engineering of solar photocatalytic collectors. Sol. Energy 77, 513–524. https://doi.org/10.1016/j.solener.2004.03.020.

Malato, S., Fernández-Ibáñez, P., Maldonado, M.I., Blanco, J., Gernjak, W., 2009. Decontamination and disinfection of water by solar photocatalysis: recent overview and trends. Catal. Today 147, 1–59. https://doi.org/10.1016/J.CATTOD.2009.06.018.

Martín-Sómer, M., Pablos, C., van Grieken, R., Marugán, J., 2017. Influence of light distribution on the performance of photocatalytic reactors: LED vs mercury lamps. Appl. Catal. B Environ. 215, 1–7. https://doi.org/10.1016/j.apcatb.2017.05.048.

Martín-Sómer, M., Vega, B., Pablos, C., van Grieken, R., Marugán, J., 2018. Wavelength dependence of the efficiency of photocatalytic processes for water treatment. Appl. Catal. B Environ. 221, 258–265. https://doi.org/10.1016/J.APCATB.2017.09.032.

Martín-Sómer, M., Pablos, C., de Diego, A., van Grieken, R., Encinas, Á., Monsalvo, V.M., Marugán, J., 2019. Novel macroporous 3D photocatalytic foams for simultaneous wastewater disinfection and removal of contaminants of emerging concern. Chem. Eng. J. 366, 449–459. https://doi.org/10.1016/J.CEJ.2019.02.102.

McGuigan, K.G., Samaiyar, P., du Preez, M., Conroy, R.M., 2011. High compliance randomised controlled field trial of solar disinfection of drinking water and its impact on childhood diarrhea in rural Cambodia. Environ. Sci. Technol. 45, 7862–7867. https://doi.org/10.1021/es201313x.

Meierhofer, R., Landolt, G., 2009. Factors supporting the sustained use of solar water disinfection - experiences from a global promotion and dissemination programme. Desalination 248, 144–151. https://doi.org/10.1016/j.desal.2008.05.050.

Miralles-Cuevas, S., Oller, I., Agüera, A., Sánchez Pérez, J.A., Sánchez-Moreno, R., Malato, S., 2016. Is the combination of nanofiltration membranes and AOPs for removing microcontaminants cost effective in real municipal wastewater effluents? Environ. Sci. Water Res. Technol. https://doi.org/10.1039/C6EW00001K.

Ogbonna, J.C., Soejima, T., Tanaka, H., 1999. An integrated solar and artificial light system for internal illumination of photobioreactors. Elsevier, 289–297 https://doi.org/10.1016/s0079-6352(99)80121-0.

Ogbonna, J.C., Soejima, T., Ugwu, C.U., Tanaka, H., 2001. An integrated system of solar light, artificial light and organic carbon supply for cyclic photoautotrophic-heterotrophic cultivation of photosynthetic cells under day-night cycles. Biotechnol. Lett. 23, 1401–1406. https://doi.org/10.1023/A:1011693606473.

OMS/UNICEF, 2017. Progress on drinking water, sanitation and hygiene: 2017 update report and SDG baseline.

Pablos, C., Marugán, J., van Grieken, R., Adán, C., Riquelme, A., Palma, J., 2014. Correlation between photoelectrochemical behaviour and photoelectrocatalytic activity and scaling-up of P25-TiO2 electrodes. Electrochim. Acta 130, 261–270. https://doi.org/10.1016/j.electacta.2014.03.038.

Philippe, K.K., Timmers, R., Van Grieken, R., Marugan, J., 2016. Photocatalytic disinfection and removal of emerging pollutants from effluents of biological wastewater treatments, using a newly developed large-scale solar simulator. Ind. Eng. Chem. Res. 55, 2952–2958. https://doi.org/10.1021/acs.iecr.5b04927.

Rose, A., Roy, S., Abraham, V., Holmgren, G., George, K., Balraj, V., Abraham, S., Muliyil, J., Joseph, A., Kang, G., 2006. Solar disinfection of water for diarrhoeal prevention in southern India. Arch. Dis. Child. 91, 139–141. https://doi.org/10.1136/adc.2005.077867.

Sánchez Pérez, J.A., Román Sánchez, I.M., Carra, I., Cabrera Reina, A., Casas López, J.L., Malato, S., 2013. Economic evaluation of a combined photo-Fenton/MBR process using pesticides as model pollutant. Factors affecting costs. J. Hazard. Mater. 244–245, 195–203. https://doi.org/10.1016/j.jhazmat.2012.11.015.

Seider, W., Seader, J., Lewin, D., 2004. Product & Process Design Principles: Synthesis, Analysis and Evaluation. John Wiley and Sons, New York.

United Nations General Assembly, 2010. Resolution 64/292. The human right to water and sanitation.

van Grieken, R., Marugán, J., Sordo, C., Pablos, C., 2009. Comparison of the photocatalytic disinfection of E. coli suspensions in slurry, wall and fixed-bed reactors. Catal. Today 144, 48–54. https://doi.org/10.1016/j.cattod.2008.11.017.

Zheng, Q., Aiello, A., Choi, Y.S., Tarr, K., Shen, H., Durkin, D.P., Shuai, D., 2020. 3D printed photoreactor with immobilised graphitic carbon nitride: a sustainable platform for solar water purification. J. Hazard. Mater. 399, 123097. https://doi.org/10.1016/j.jhazmat.2020.123097.